Systems and Computers in Japan, Vol. 34, No. 2, 2003
Translated from Denshi Joho Tsushin Gakkai Ronbunshi, Vol. J83-D-II, No. 10, October 2000, pp. 2017–2029

Contour Extraction of Left Ventricular Cavity from Digital Subtraction Angiograms Using a Neural Edge Detector

Kenji Suzuki,[1,*] Isao Horiba,[1] Noboru Sugie,[2] and Michio Nanki[3]

[1]Faculty of Information Science and Technology, Aichi Prefectural University, Aichi, 480-1198 Japan

[2]Faculty of Science and Technology, Meijo University, Nagoya, 468-8502 Japan

[3]Division of Cardiovascular Medicine, Chubu Rosai Hospital, Nagoya, 455-0018 Japan

SUMMARY

In this paper, a supervised edge detector based on a multilayer neural network, which is called a neural edge detector (NED), is proposed for detecting edges which coincide with edges traced by a human operator (e.g., a medical doctor). The NED is trained by use of the contours traced by a cardiologist. Using the trained NED, the contours coinciding well with the contours traced by a cardiologist are extracted from the left ventricular angiograms even with nonuniform contrast medium.

The proposed contour extraction method consists of (1) detection of fine edges by the NED, (2) extraction of rough contours, and (3) contour tracing based on contour candidates synthesized from the rough contours and the edges detected by the NED. The contour of the left ventricle is automatically extracted by inputting two points manually. Experiments with clinical images show that the proposed method can stably extract the contours coinciding well with the contours traced by a cardiologist. © 2003 Wiley Periodicals, Inc. Syst Comp Jpn, 34(2): 55–69, 2003; Published online in Wiley InterScience (www.interscience.wiley.com). DOI 10.1002/scj.1190

Key words: supervised edge detection; contour extraction; image enhancement; nonuniform contrasting; neural filter.

1. Introduction

Contour extraction of the left ventricle in DSA (digital subtraction angiography) is one of the most fundamental and important operations to obtain functional information on the heart, such as the left ventricular volume. Since there is a strong need to automate this work, various methods for performing it have been proposed [1–7]. In contrasting the left ventricle in DSA, the contrast in the left ventricle is often nonuniform because the contrast medium (a substance with a high X-ray absorption coefficient infused to enhance the contrast of an image) cannot be used in a large quantity due to stress on the patient, the contrast medium may be diluted due to blood flow from the mitral valve, and the flow is disturbed due to the complicated structures within the left ventricle. Thus, it is very difficult to extract the contours automatically and stably. In clinical applica-

*Presently at the Kurt Rossmann Laboratories for Radiologic Image Research, Department of Radiology, The University of Chicago, Chicago, Illinois 60637, USA.

Contract grant sponsor: Supported in part by the Ministry of Education, Science, Sports, and Culture of Japan under a grant-in-aid for quantum information theoretical approach to life science and a grant-in-aid for encouragement of young scientists.

tions, parts of a contour which do not coincide with the judgment of a cardiologist in the automatically extracted contour are corrected manually. Therefore, development of a method for extracting a contour which coincides well with the contour based on a medical doctor's judgment is highly desirable. This can be technically realized if such a judgment algorithm can be described explicitly as procedures or a program. Since it cannot be clearly expressed even by a specialist (e.g., a medical doctor), realizing this task is very difficult and no studies on such contour extraction have been reported yet. The purpose of this study is to develop a method for extracting contours which coincide well with the judgment of a cardiologist.

A number of methods for images other than DSA have been proposed for extracting the contour of the left ventricle. These include methods for US (ultrasonic) images [8–12], methods for X-ray CT (computed tomographic) images or MR (magnetic resonance) images [13–17], and methods for nuclear medical images [18–20]. These methods consist of detection of the edges of a contour and integration of the edges as a contour. Since US images are images with poor signal-to-noise ratios, an edge detector that is robust against noise and an integration method have been used in researches for US images. Because CT and MR images are comparatively clear images, the methods are based on a simple edge detector, thresholding, or morphological characteristic extraction. Since nuclear medical images are images with generally unclear contours, an image segmentation method is often used for this kind of image. Those methods can extract contours well. However, all of those methods do not actively extract contours which coincide well with the contours traced by a medical doctor.

In recent years, neural filters (NF), which are nonlinear filters based on multilayer neural networks (NN) that have a learning capability and a highly nonlinear processing capability, have been proposed in the field of signal processing [21–24]. An NF can realize image processing with a desired function by training with input images together with ideal teaching images. In this paper, we expand a capability of an NF, and propose a supervised edge detector called a neural edge detector (NED) for extracting a contour which coincides well with the contour traced by a cardiologist.

Although various edge detection algorithms have been proposed [25–28], no algorithms for extracting edges traced by a human operator (e.g., a medical doctor) have been proposed. In addition, although the following three kinds of studies of the application of an NN to the edge detection problem have been made, they could not detect the edges traced by a human:

(1) edge detection based on a cellular NN that is constructed by combining simple cells as in the retina [e.g., 29–31];

(2) edge detection based on a self-organizing map [e.g., 32–35];

(3) edge detection based on a Hopfield network [e.g., 36–39].

In addition, studies to extract a boundary between an organ and others have been performed. In those studies, extraction of a boundary was treated as an image segmentation problem, and a neural classifier that is applied in the field of character recognition was used. References 40 and 41 present examples of applications to medical images. In such an NN, image features such as a histogram of a local region is input and the class to which an image belongs, such as the name of the tissue, is output. This NN does not extract edges and cannot handle analog values such as fluctuations in tracing by a human.

In this study, an attempt is made to extract a contour which coincides well with the contour traced by a cardiologist from a left ventricular angiogram with nonuniform contrast medium, obtained by use of a relatively small amount of contrast medium, by using an NED capable of training the contours traced by a cardiologist. The proposed contour extraction method consists of (1) detection of fine edges by the NED, (2) extraction of a rough contour, and (3) contour tracing based on contour candidates synthesized from the rough contours and the edges detected by the NED. The effectiveness of the proposed method is evaluated by experiments with left ventricular angiograms at end-diastole.

2. Contour Extraction Method

The proposed method is illustrated in Fig. 1. This method includes (1) use of an NED to detect edges which coincide well with the contour traced by a cardiologist, (2) extraction of a rough contour, and (3) tracing of a contour on the basis of contour candidates synthesized from the edges detected by the NED and the rough contours.

2.1. Edge detection by NED

2.1.1. Architecture of NED

The NED is a supervised edge detector based on a multilayer NN. In the NN, it is appropriate to use a linear function instead of a nonlinear function as an activation function of the output layer unit of the NN [42] when handling continuous values such as the edges in an image. Consequently, the structure of the NED is such that an identity function, sigmoid function, and linear function is used as the activation function of each unit in the input, hidden, and output layers. The inputs of the NED are pixel values in a local region, that is, the object pixel value $g(x, y)$ and the neighboring pixel values, and the output of the

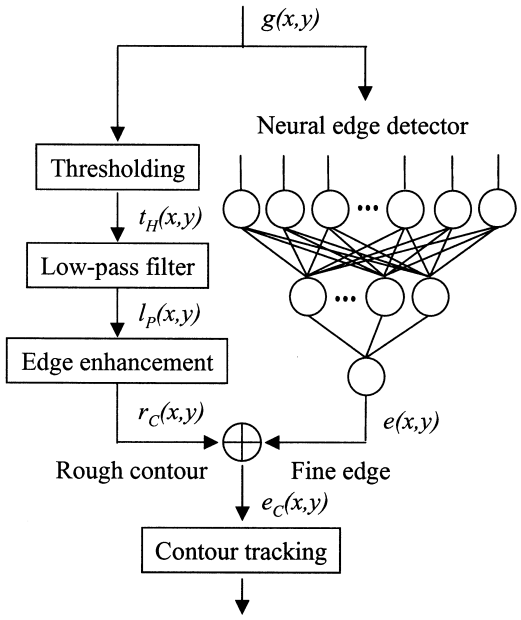

Fig. 1. Method for extracting the contour of the left ventricular cavity.

NED is edge information $e(x, y)$ corresponding to the center pixel in the local region, as represented by the following equations:

$$e(x, y) = NN(\boldsymbol{I}_{x,y}) \tag{1}$$

$$\boldsymbol{I}_{x,y} = \{g(x - i, y - j)|i, j \in R_S\} \tag{2}$$

where $\boldsymbol{I}_{x,y}$ is an input vector at (x, y), $NN(\boldsymbol{I})$ is the output of the multilayer NN having $\boldsymbol{I}$ as an input vector, and R_S is the local region of the multilayer NN.

2.1.2. Training of NED

The NED learns the relationship between an input image and a teaching image which contains ideal edges by adjusting the weights of the NED. The error function for training is defined by

$$E = \sum_{p} (T_C^p - O^p)^2 \tag{3}$$

where T_C^p is the p-th pixel value in the training region in the teaching images, and O_p is the p-th pixel value in the training region in the output image. Training is performed by means of a modified back-propagation algorithm in Ref. 42 for the above structure of the NN, which was derived in the same manner as the back-propagation algorithm [43].

In order to extract a contour stably, the following image is used as the input image to the NED $g(x, y)$: an image obtained by subtracting a left ventricular angiogram before contrasting with the contrast medium from that after contrasting [44]. The disturbing effects of the organs and bones surrounding the heart can be reduced by such preprocessing. The contour traced by a cardiologist is used to make the teaching image for the NED. The contour traced by the cardiologist is not accurately represented by one curve, it contains a sort of an error (fluctuation), and it constitutes the center of the distribution of the probability where the contour exists.

Assuming that this distribution is a normal distribution, the teaching image can be obtained by performing a Gaussian filter on the contour traced by the cardiologist, represented by

$$T_C(x, y) = C_D(x, y) * G(x, y; \sigma) \tag{4}$$

where $C_D(x, y)$ is an image that includes the contour traced by the cardiologist, $G(x, y; \sigma)$ is a Gaussian function with the standard deviation σ, and * is the convolution operator. In addition, this teaching image is normalized in such a way that the minimum value and the maximum value is the minimum value of the gray scale L_{MIN} and the maximum value of the gray scale L_{MAX}, respectively. The NED is expected to output edges coinciding well with the contour traced by the cardiologist by training these input images and teaching images that expresses the distribution for confidence of the edges.

2.2. Rough contour extraction

(1) Thresholding

Threshold selection is performed by Otsu's method [45] on an input image $g(x, y)$, and binarization into L_{MIN} and L_{MAX} is performed as in the following equations:

$$t_H(x, y) = \begin{cases} L_{MAX} & if\ g(x, y) \geqq th \\ L_{MIN} & if\ g(x, y) < th \end{cases} \tag{5}$$

where th is a threshold value.

(2) Low-pass filtering

Low-pass filtering is performed on the binary image by means of a Hamming window as expressed by the equation

$$l_P(x, y) = \phi^{-1}[\phi\{t_H(x, y)\} \cdot h(R_H)] \tag{6}$$

where $\phi(\cdot)$ and $\phi^{-1}(\cdot)$ are the Fourier transform and inverse Fourier transform operators, $h(R_H)$ is a Hamming function

with a window diameter of R_H, and R_H is the factor governing the width of the rough contour.

(3) Edge enhancement

Edge enhancement is performed on the low-pass-filtered image by use of a Sobel filter [47] as follows:

$$r_C(x, y) = \psi\{l_P(x, y)\} \tag{7}$$

where $\psi(\cdot)$ is the Sobel filtering operator. The output image $r_C(x, y)$ has the approximate contour extracted.

2.3. Contour tracing

A contour candidate image is obtained by synthesizing the rough contour image $r_C(x, y)$ and the edges detected by the NED $e(x, y)$:

$$e_C(x, y) = r_C(x, y) + e(x, y) \tag{8}$$

We give a start point and an end point to the contour tracing method. These two points are near the mitral valve–aortic root junction and the junction of aortic root and anterior endocardium. Then, contour tracing is applied to the contour candidate image.

A scheme [48] developed to trace blood vessels was simplified and used for contour tracing. First, consider a vector of a certain length r extending radially outward from the object point P. As shown by the following equation, the average gray level of the pixels on the vector in a certain direction θ is obtained:

$$g_S(\theta) = \sum_{x,y \in R_{P,\theta}} e_C(x, y)/r \tag{9}$$

where $R_{P,\theta}$ is the coordinates on the vector having a object point P and forming an angle θ with the x axis. Consider the orientation from the previously traced direction for the average gray level on the vector as follows:

$$g_C(\theta) = g_S(\theta) \cdot w_f(\theta - D) \tag{10}$$

where D is the previously traced direction and $w_f(\cdot)$ is a weighting function giving the preceding orientation, expressed by

$$w_f(u) = 1 - \left(\frac{u}{w_D \pi}\right)^2 \tag{11}$$

where w_D is a parameter determining the search range. Using the average gray level on the vector with consideration of the previous orientation, the direction with maximum average gray level is chosen as the tracing direction as follows:

$$D_M = \theta : \max_{\theta}\{g_C(\theta)\} \quad (D - w_D\pi \leqq \theta \leqq D + w_D\pi) \tag{12}$$

The end point P_M of the vector of the tracing direction D_M obtained thus is chosen as the tracing point. Sequential tracing is performed by reading the tracing point P_M as the object point P and the tracing direction D_M as the previously traced direction D. Tracing is stopped when the following condition is fulfilled: $\max_\theta\{g_C(\theta)\} - L_{MIN}$ less than or equal to 5% of $L_{MAX} - L_{MIN}$. The contour of the left ventricle is obtained by combining the traced lines at the crossing points, with tracing begun in both directions from the given two points.

3. Comparative Evaluation of the Performance on Edge Detection of NED

The performance on edge detection of the NED and conventional edge detectors are evaluated comparatively with respect to their performance on detecting the edges close to those traced by a cardiologist.

3.1. Comparison of detected edges

An example of training images for the NED is shown in Fig. 2. Image (a) is an angiogram of the left ventricle at end-diastole (512×480 pixels, 1024 gray levels) in the 30° right anterior oblique projection, obtained with a digital X-ray imaging system (DSA-100, Hitachi Medical, Kashiwa, Japan). Since this image is contrasted by the contrast medium administered in a relatively small quantity, the gray levels are not uniform. In addition, the contrast medium is diluted due to blood flow from the mitral valve. Thus, there are a number of places where the contour is vague. However, an experienced cardiologist can extract a contour in such places on the basis of his or her medical knowledge. Image (b) is the teaching image obtained by means of Eq. (4) from the contour traced by the cardiologist. This contour is carefully traced from the image obtained at end-diastole and images before and after this image. In Refs. 3 and 49, the reproducibility of the contour traced by a cardiologist was evaluated by having a number of cardiologists extract the same image multiple times. Since the evaluations were made in regulated situations, the results almost entirely coincide with the fluctuations in the carefully obtained contours. Since σ was 1.0 to 1.5 when these fluctuations were approximated by a normal distribution, the center of these values was used as σ in Eq. (4).

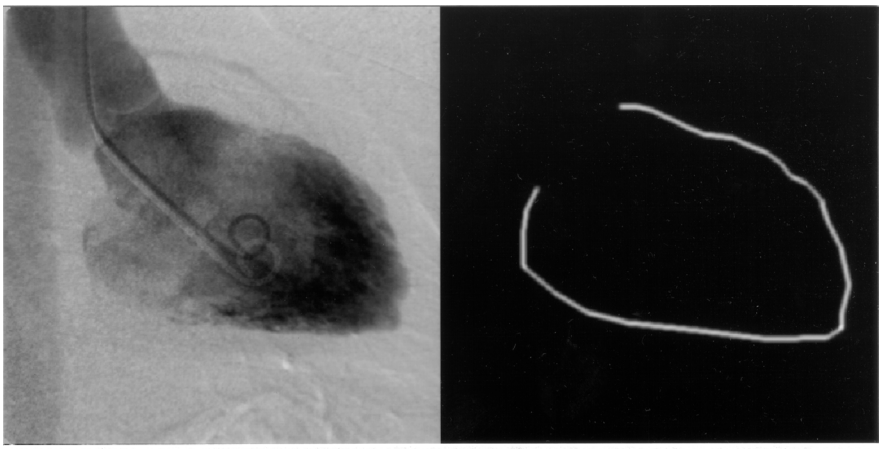

(a) Input image. (b) Teaching edge made from the contour traced by a medical specialist.

Fig. 2. Sample of the images used for training.

The NED is trained with these images to obtain the function to detect the contours that coincide well with the contours traced by a cardiologist from left ventricular angiograms with nonuniform contrast medium. A region sufficiently covering the contour in the teaching image was used as the training region. Three-layered NED was trained by use of the training algorithm with optimization of structure in Refs. 50 and 51. The use of three-layered NED is theoretically appropriate, since it has been proved in Refs. 52 and 53 that a three-layered multilayer NN can approximately realize arbitrary continuous mapping with an arbitrary accuracy. As a result of applying the optimization algorithm, a region consisting of 81 pixels with the object pixel at the center was selected as the input layer, 10 units were used as the hidden layer, and the training was converged with an average absolute error (normalized by use of L_{MAX}) of 19.9%.

The performance of the trained NED and that of conventional edge detectors is comparatively evaluated.

Conventional edge detectors can be classified into the following three categories [54]:

1) edge detectors based on gray-level derivatives in a local region;

2) edge detectors obtained with an assumption that edge detection is treated as an optimal filtering problem;

3) edge detectors based on an edge model.

The Sobel filter [47], the Marr–Hildreth operator [55], and the Hueckel operator [56] are representative methods of categories 1), 2), and 3), respectively. Since the conventional edge detectors are based on certain edge models, the edges detected by them do not necessarily coincide with the edges traced by a cardiologist. On the other hand, since a multilayer NN is a model which can realize an arbitrary mapping approximately [52, 53], the NED using such a network has a large degree of freedom, which comes from the possibility of designing all weights by training, and thus it has a large model capacity. Thus, it can detect edges which coincide well with the contour traced by a cardiologist.

To compare fairly, the parameters of each edge detector were optimized by use of the error function in Eq. (3). Here, the Sobel filter was applied unaltered, because there are no parameters associated with the Sobel filter. Figure 3 shows comparisons of the output images of the NED and the conventional edge detectors. In the output images of the conventional detectors, many edges are detected by mistake because of the following factors: the flow is disturbed due to the complicated structures within the left ventricle, contrast medium is nonuniform, and edges of the contour are unclear due to diluted contrast medium. In contrast, in the output image of the NED, the contour is detected as continuous edges. This contour coincides relatively well with that traced by the cardiologist. This shows that the NED is not affected by the nonuniformity of contrast medium.

Here, we discuss the edge detection results by the NED. It is considered that when a cardiologist traces a contour from a left ventricular angiogram, he or she determines the border between the area in which the contrast medium is present, even in a small amount, and the area in which no contrast medium is present, based on anatomical knowledge of the shape of the left ventricle. Since the NED uses only information within local areas, the anatomical knowledge of the cardiologist is not learned while training

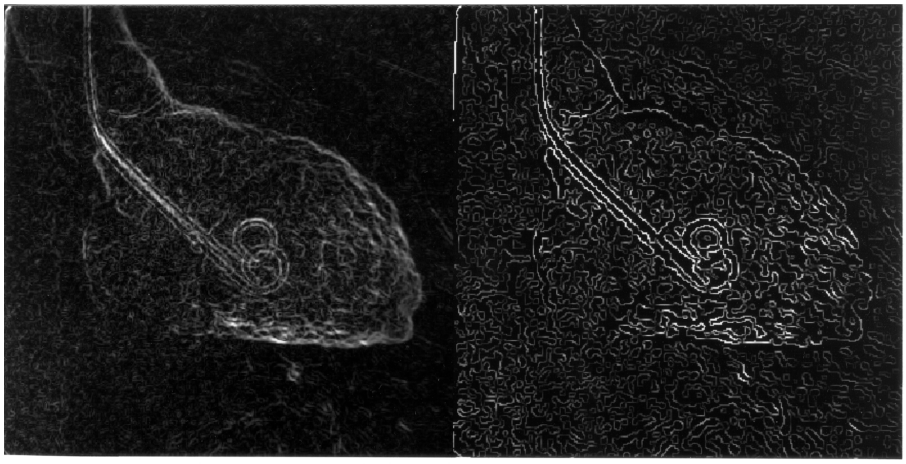

(a) Output image of the Sobel filter.

(b) Output image of the optimal Marr-Hildreth operator.

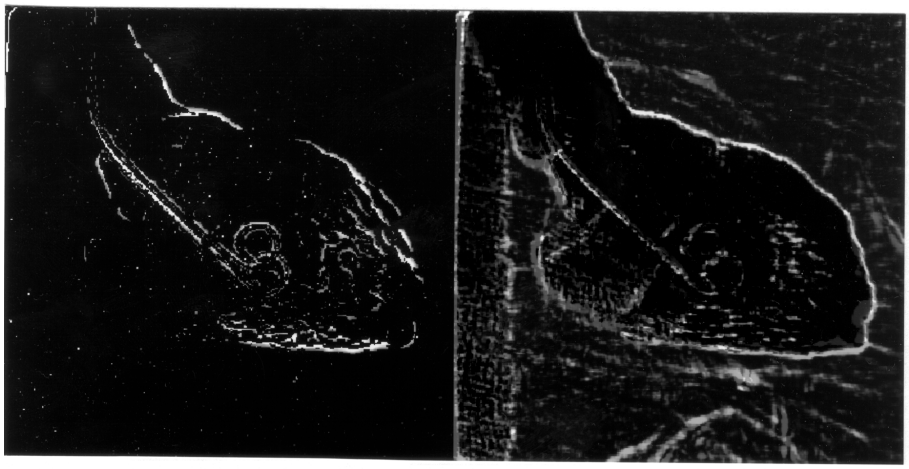

(c) Output image of the optimal Hueckel operator.

(d) Output image of the neural edge detector.

Fig. 3. Comparison of the edges detected by the neural edge detector with those detected by the conventional edge detectors.

the contour traced by the cardiologist. Since the NF having the same structure as the NED shows nonlinear characteristics with respect to the gray levels within the input local region [57, 58], the NED is considered to be capable of adaptive processing in response to the gray levels within the input local region. Since the input image is a subtraction image before and after contrasting, the occurrence of an almost constant gray level of the area in which no contrast medium exists is taken to be a characteristic of edge detection. It thus can be inferred that the NED learns in such a way that the borderline between the area in which the contrast medium exists and the area in which no contrast medium exists is output as edge information, with the gray levels within the input local region as indices. In order to support this reasoning, elucidating edge detection by the NED by analyzing its learning would be an important future task.

3.2. Comparative evaluation of edge detection performance in nontraining images

Since the NED is a supervised edge detector, its evaluation on nontraining images is important. Evaluations were made by use of a cross validation (a method of dividing a data set into a set for training and a set for testing, making cross evaluations of all sets while changing these sets sequentially; it is often used to verify the performance of the training mechanism such as a neural network). With this method, a maximum number of evaluations can be guaranteed for a small number of cases. Two cases from typical left ventricular angiograms at end-diastole out of five cases (512×480 pixels, 1024 gray levels) were used as the set for training and the remaining three cases were used for the set for testing. Thus, the number of training NEDs was ${}_5C_2 = 10$, the total number of images tested was

Table 1. Comparison of the error between the edges detected by each edge detector and that detected by a medical doctor

	Sobel filter	Optimal Marr-Hildreth operator	Optimal Hueckel operator	Neural edge detector
Max. value	0.31	0.36	0.34	0.30
Mean value	0.30	0.33	0.33	0.22
Min. value	0.29	0.32	0.31	0.11

$5 \times 10 = 50$, and the number of nontraining images tested among these was $3 \times 10 = 30$. When the NED was trained by use of the training method with optimization of the structure described above, from 68 to 81 units were selected for the input layer, from 7 to 12 units were selected for the hidden layer. The trainings were converged with average absolute errors from 19.9 to 22.4%. The parameters of the conventional edge detectors were optimized in the same way as in the previous section in order to obtain the highest performance for these cases.

The error between the edges $e(x, y)$ detected by each edge detector and the teaching edges $T_C(x, y)$ was calculated by use of Eq. (3). The minimum value, the mean value, and the maximum value of the error for 30 nontraining images used for evaluations are shown in Table 1. The errors of the NED are smaller than those of the conventional edge detectors. The generalization ability (performance for nontraining cases) of the NED is the highest in terms of the characteristic of detecting edges close to the contour traced by the cardiologist.

4. Experimental Evaluation of Contour Extraction Performance of the Proposed Method

The proposed contour extraction method was also evaluated from the points of view of degree of coincidence with the contour traced by the cardiologist, and stability of the method.

4.1. Examples of contour extraction results

The results $r_C(x, y)$ of extracting a rough contour for Fig. 2 are shown in Fig. 4(a). The rough contour image is used for tracing the contour stably by reinforcing the edges detected by the NED. Thus, the parameter R_H with respect to the low-pass filter was set in such a way that a rough contour whose width sufficiently covers the left ventricular contour can be extracted. The contour was traced by specifying two points on the basis of the contour candidates $e_C(x, y)$ that was obtained by synthesizing the rough contour and the edges detected by the NED. The results are shown in Fig. 4(b) by superposition with the contour candidates. In addition, W_D, which is a parameter expressing the previous orientation of tracing, was set at 0.35 (the order of 0.3 to 0.4 is stable for a tracing problem in which there are few rapid changes, as in the contour of the left ventricle), so that 70% is the search range, with r corresponding to the contour tracing step of 15 pixels (the order of 10 to 20 pixels is stable for images of this size). The results reveal that the left ventricular contour could be traced accurately. The image obtained by superimposing the contour obtained by the proposed method and the contour traced by the cardiologist is shown in Fig. 4(c). The contour obtained by the proposed method coincides very accurately with the contour traced by the cardiologist.

4.2. Quantitative evaluations of the generalization ability with non-training images

As in the comparative evaluations of the edge detection performance, the generalization ability of the proposed contour extraction method was evaluated quantitatively by use of the cross-validation test. First, the valve part of the contour obtained by the cardiologist and that obtained by the proposed method were closed and a left ventricle area image with the left ventricle area as one and the other areas as zero was created. As an evaluation index expressing the difference of the two contours, the contour error is defined as follows:

$$E_C = \frac{\sum_{x,y} \{a_P(x, y) \oplus a_D(x, y)\}}{\sum_{x,y} a_D(x, y)} \tag{13}$$

where $\oplus$ represents the XOR operator, and $a_P(x, y)$ and $a_D(x, y)$ represent the left ventricle area image obtained by the proposed method and that obtained from the contour traced by the cardiologist. In addition, since the contour of the left ventricle is used for calculating the volume of the left ventricle, evaluations by the area error of the following equation are also important:

$$E_A = \frac{\sum_{x,y} a_D(x, y) - \sum_{x,y} a_P(x, y)}{\sum_{x,y} a_D(x, y)} \tag{14}$$

The results of calculating the contour error and the area error are shown in Table 2. The minimum value, mean value, maximum value, and standard deviation of the contour error for 30 nontraining images are shown. It can be

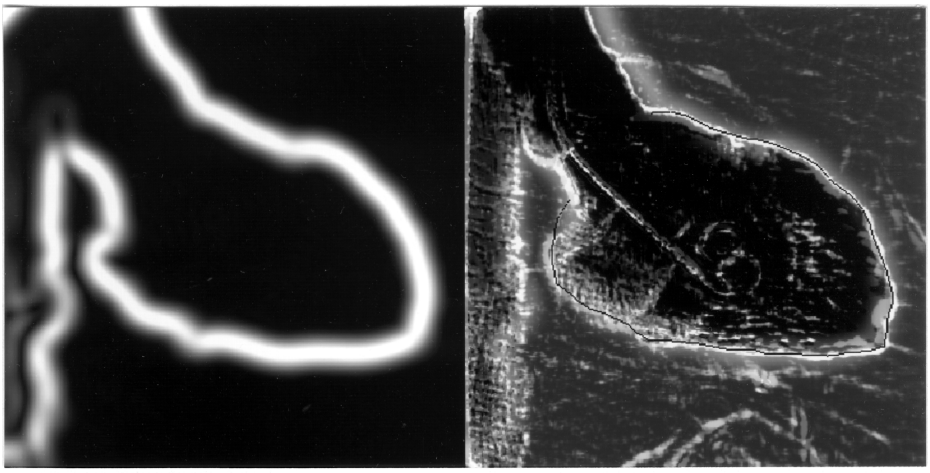

(a) Result of the extraction of rough contours.

(b) Image of candidates for the contours, which is overlaid with the result of the contour tracking.

(c) Comparison of the contour extracted by the proposed method, indicated by a black curve, with that traced by a medical specialist, indicated by a white curve.

Fig. 4. Result of the extraction of the contour.

Table 2. Normalized error between the contour extracted by the proposed method and that extracted by a medical doctor

	E_C	E_A
Max. value	12.4%	12.4%
Mean value	7.6%	6.0%
Min. value	3.6%	0.7%
SD	2.6%	3.1%

SD: Standard deviation

seen that the average error and the maximum error are small and that extraction of a contour close to that of the cardiologist can be realized by the proposed method, indicating the generalization ability of the proposed method. The standard deviation is also small, indicating that the contour was extracted by the proposed method stably.

The contour candidate image which serves as the basis for contour tracing is now discussed. In order to differentiate the effects of the edge image obtained by the NED and the rough contour image, contour tracing was performed on the basis of only the rough contour image. The results of calculating the error in this case are shown in

Table 3. Normalized error between the contour extracted with only the rough contour or only the edges detected by the NED and that extracted by a medical doctor

	Rough contour		NED	
	E_C	E_A	E_C	E_A
Max. value	12.9%	12.4%	33.4%	25.3%
Mean value	10.0%	8.9%	11.3%	8.5%
Min. value	6.6%	5.0%	2.5%	1.5%
SD	3.0%	3.1%	8.1%	6.5%

SD: Standard deviation

Table 3. It can be seen that the edge image obtained by the NED shows a contour closely approximating the contour traced by the cardiologist. In addition, the results of tracing the contour on the basis of only the edge image obtained by the NED showed that the tracing was indefinite (judged by the visual basis) in 11 of 50 images, which were all non-training images. The results of calculating the error in 19 successfully traced nontraining images are shown in Table 3. One reason that the results based on the NED alone are not better than the results based on the rough contour image alone is that the contour tracing process is not robust against the interruptions of the edges. As shown in Fig. 3(d), there are interrupted parts in the edges, although the edge image obtained by the NED coincides well with the contour traced by the cardiologist. When there are such parts, tracing is indefinite and tends to be unstable. Since there are no interrupted parts in the rough contour image as shown in Fig. 4(a), tracing is definite. It can be seen from the above results that the ability of the proposed method to extract comparatively stably a contour close to the contour traced by the cardiologist is due to the complementary effect of the synthesis of the two images, and that the rough image contributes to stabilizing the contour tracing in later stages, while the image of the edges detected by the NED functions to approximate closely the contour traced by the cardiologist.

Among the contour extraction results, two cases showing the smallest contour errors and two cases showing the largest contour errors are given in Figs. 5 to 8. In Fig. 6, the method traces a part of a hemostat clip erroneously, although it shows an overall contour which is close to the contour traced by the cardiologist. In Fig. 8 which represents the worst case with the greatest contour error, the edges of the posterior wall (lower part) of the left ventricle in the input image are very vague. The contour obtained by the proposed method shows parts which do not coincide in such edges.

The errors associated with other methods are also discussed here. A method which incorporates some training into the contour extraction is presented in Ref. 4. This contour extraction method extracts a contour in four stages: (1) transformation into an image in a knowledge base with the heart divided into six areas, (2) search for contour candidate points, (3) contour extraction by the DP matching based on multiple evaluation functions, (4) correction of the contour by a heart model composed of multiple templates, by inputting four points (two points of the posterior edge

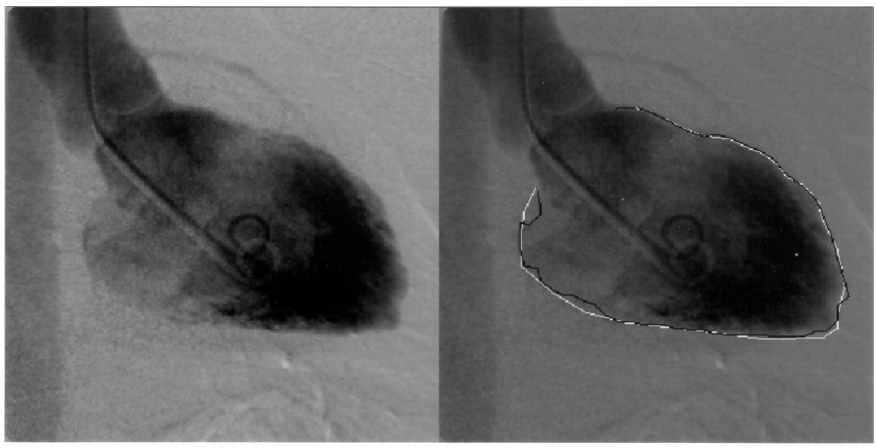

(a) Input image.

(b) Comparison of the contour extracted by the proposed method with that traced by a medical specialist.

Fig. 5. Result of the extraction of the contour in the best case (E_C = 3.6%)..

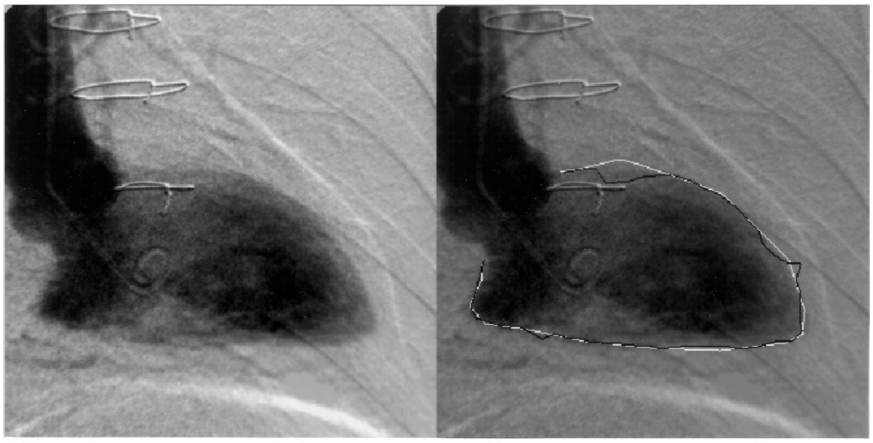

(a) Input image.

(b) Comparison of the contour extracted by the proposed method with that traced by a medical specialist.

Fig. 6. Result of the extraction of the contour in the second best case ($E_C = 4.0\%$)..

of the mitral valve ring and the heart apex in addition to the two points of the proposed method). It has been reported that when the heart model of point (4) was trained by using 50 images and 25 images were then evaluated, the contour error E_C was 10.1% on average and the standard deviation was 7.2% in the best cases among the cases produced by varying various parameters. It is seen that the proposed method can extract a contour close to the contour traced by a cardiologist, indicating that it is a stable method, as compared with the method discussed above.

In addition, the relationships between the variations in the contour traced by a cardiologist and the contour extracted by the proposed method are discussed here. Reference 59 has reported that in evaluations of only the images of a state in which the blood flow is stable, the average area error E_A of multiple cardiologists belonging to the same hospital was 2.5 to 3.1% on average. Here, the conversion from the left ventricular volume to the area error was made by the area–length method [60]. This assures good imaging conditions and reproducibility of a contour within a short time, and cases in which the error of reproducibility is very small are shown. Reference 61 has reported that the difference in the area error by cardiologists belonging to different hospitals was within 1.2%. Specifically, the variations in the contours traced by cardiologists contain this error in the numbers given above. In general, if the average area error

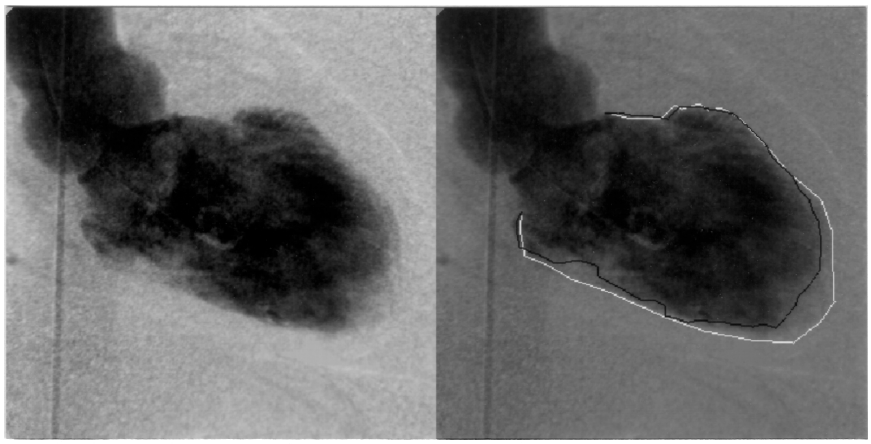

(a) Input image.

(b) Comparison of the contour extracted by the proposed method with that traced by a medical specialist.

Fig. 7. Result of the extraction of the contour in the second worst case ($E_C = 12.3\%$).

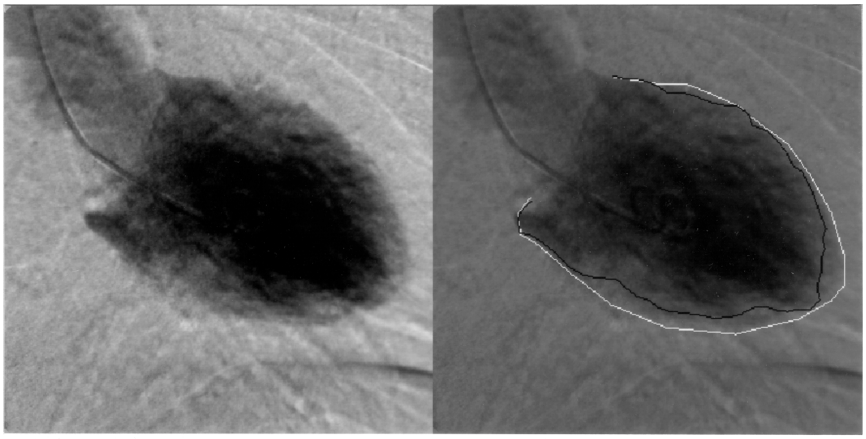

(a) Input image.

(b) Comparison of the contour extracted by the proposed method with that traced by a medical specialist.

Fig. 8. Result of the extraction of the contour in the worst case (E_C = 12.4%).

is less than 5.1% and the standard deviation is less than 2.5% with respect to the reproducibility of the contour traced by a cardiologist, this is considered to be an acceptable range which does not cause any clinical problems. Eighty-seven percent of the results extracted by the proposed method were within this range, indicating that the proposed method allows extraction of a contour equal to that traced by a cardiologist in a comparatively stable range.

4.3. Evaluations by cardiologists

On evaluating the contours extracted by the proposed method from a clinical standpoint, cardiologists determined that the contours obtained by the proposed method coincided well with those traced by a cardiologist. In addition, an edge image detected by the NED is very useful clinically, since it can be seen as an image of the distribution expressing the accuracy of the contour of the left ventricle and it tends to have a confidence level almost coinciding with the contour judged by an experienced cardiologist.

5. Conclusions

In this paper, a supervised edge detector based on a multilayer neural network, which is called a neural edge detector (NED), is proposed for detecting the edges which coincide well with a contour traced by a cardiologist, and a method for extracting the contour of the left ventricle by means of the NED is proposed. It is shown by evaluation experiments using angiograms of the left ventricle at end-diastole that the proposed method can extract a contour which coincides well with the contour obtained by a cardiologist. Quantitative evaluation of the fluctuations in tracing contours by cardiologists shows the possibility that the proposed method can extract contours equal to those traced by cardiologists in about 90% of cases. The remaining 10% of the contours need correction of parts which do not coincide.

The authors plan to evaluate the proposed method in an increased number of cases in the future in order to make further improvements. In addition, utilization of the NED gives consistency to the judgment of a cardiologist, since it can extract a contour which coincides with the judgment of a cardiologist comparatively well. The authors also plan to conduct a study to clarify the algorithm for contour extraction of a cardiologist by analyzing an NED which has been trained with the contour traced by the cardiologist. This is considered to be an important study since it is expected to be a key to understanding the logic of judgment by cardiologists during contour extraction, which is not clear to the cardiologist him- or herself. Although a contour traced by a cardiologist is given as a teaching contour in this study, physical contours may also be given by using phantoms and the like. A study of the changing of such given contours depending on uses is also being planned.

The inner wall of the left ventricle at end-systole has a complicated shape with intertwined papillary muscles. Although a cardiologist determines this contour on the basis of his or her medical knowledge and clinical experience while referring to the time series images, this is different from the edges of an image. Thus, the contour at end-systole

was not treated in this study; a method for obtaining the contour at end-systole will be developed in the future by integrating with other approaches, such as that of Snakes [62]. In addition, the proposed method will be applied to the extraction of organs having complicated shapes which have been difficult to detect by existing edge detectors.

Acknowledgments. The authors thank Professor S. Okabayashi of Meijo University, Professor S. Yamamoto of the Faculty of Science and Technology of Meijo University, Dr. K. Ueda of Nagoya Electric Works, and graduate student Y. Yoshida of Meijo University for their valuable suggestions, graduate student A. Hirase of Meijo University for her assistance, and Mr. S. Yanaka, Mr. K. Koike, Dr. K. Ishikawa, and Mr. S. Ikeda of the Research and Development Center at Hitachi Medical Corporation for their supports. This work was supported in part by the Ministry of Education, Science, Sports, and Culture of Japan under a grant-in-aid for quantum information theoretical approach to life science and a grant-in-aid for encouragement of young scientists.

REFERENCES

1. Matsuo K, Iwata A, Suzumura N, Horiba I, Takahashi M. An algorithm for detecting left ventricle boundaries oriented to digital subtraction angiographic image. Tech Rep IEICE 1984;MBE84-50.
2. Grattoni P, Bonamini R. Contour detection of left ventricular cavity from angiographic images. IEEE Trans Med Imaging 1985;4:72–78.
3. van Bree RE, Pope DL, Parker DL. Improving left ventricular border recognition using probability surfaces. Computers in Cardiology 1988. IEEE; 1989. p 121–124.
4. Lilly P, Jenkins J, Bourdillon P. Automatic contour definition on left ventriculograms by image evidence and a multiple template-based model. IEEE Trans Med Imaging 1989;8:173–185.
5. Fan N, Denys BG, Li CC, Reddy PS. Automated left ventricular border determination in cineangiograms based on a dynamic spider model. Computers in Cardiology 1990. IEEE; 1991. p 439–442.
6. Eiho S. Iyo Gazo Shori (Medical image processing). Asakura Shoten; 1992. p 108–115.
7. Demi A. New approach to automatic contour detection from image sequences: An application to ventriculographic images. Computers Biomed Res 1994;27:157–177.
8. Chu CH, Delp EJ, Buda AJ. Detecting left ventricular endocardial and epicardial boundaries by digital two-dimensional echocardiography. IEEE Trans Med Imaging 1988;7:81–90.
9. Detmer PR, Bashein G, Martin RW. Study of Perioperative Ischemia Research Group. Matched filter identification of left-ventricular endocardial borders in transesophageal echocardiograms. IEEE Trans Med Imaging 1990;9:396–404.
10. Feng J, Lin W-C, Chen C-T. Epicardial boundary detection using fuzzy reasoning. IEEE Trans Med Imaging 1991;10:187–199.
11. Abdellaoui M, Petit E, Lemoine J. Edge dynamical model applied to ventricular boundary detection on echocardiographic images. Computers in Cardiology 1991. IEEE; 1992. p 485–488.
12. Mikic I, Krucinski S, Thomas JD. Segmentation and tracking in echocardiographic sequences: Active contours guided by optical flow estimates. IEEE Trans Med Imaging 1998;17:274–284.
13. Philip KP, Dove EL, McPherson DD, Chandran KB. Automatic detection of left ventricular endocardium in cardiac images. Computers in Cardiology 1990. IEEE; 1991. p 443–446.
14. Faber TL, Stokely EM, Peshock RM, Corbett JR. A model-based four-dimensional left ventricular surface detector. IEEE Trans Med Imaging 1991;10:321–329.
15. Guttman MA, Prince JL, McVeigh ER. Tag and contour detection in tagged MR images of left ventricle. IEEE Trans Med Imaging 1994;13:74–87.
16. Ranganath S. Contour extraction from cardiac MRI studies using snakes. IEEE Trans Med Imaging 1995;14:328–338.
17. Zimmer Y, Akselrod S. An automatic contour extraction algorithm for short-axis cardiac magnetic resonance images. Med Phys 1996;23:1371–1379.
18. Duncan JS. Knowledge directed left ventricular boundary detection in equilibrium radionuclide angiography. IEEE Trans Med Imaging 1987;6:325–336.
19. Boudraa AE, Mallet JJ, Besson JE, Bouyoucef SE, Champier J. Left ventricle automated detection method in gated isotopic ventriculography using fuzzy clustering. IEEE Trans Med Imaging 1993;12:451–465.
20. Boudraa AE, Arzi M, Sau J, Champier J, Hadj-Moussa S, Besson JE, Sappey-Marinier D, Itti R, Mallet JJ. Automated detection of the left ventricular region in gated nuclear cardiac imaging. IEEE Trans Biomed Eng 1996;43:430–437.
21. Arakawa K, Harashima H. Design of layered-neural nonlinear filters using back-propagation algorithm. Trans IEICE 1991;J74-A:421–429.

22. Arakawa K, Yamakawa K, Koyama M. Neural net-type filter with optimization of its nonlinear function. Trans IEICE 1995;J78-A:151–160.
23. Suzuki K, Horiba I, Sugie N, Nanki M. Noise reduction of medical X-ray image sequences using a neural filter with spatiotemporal inputs. Proc Int Symp Noise Reduction for Imaging & Communication Systems, p 85–90, Tokyo, 1998.
24. Suzuki K, Hayashi T, Ikeda S, Horiba I, Sugie N, Nanki M. Improving image quality of medical low-dose X-ray image sequences using a neural filter. Trans IEE Japan 1999;119-C:1383–1391.
25. Gudmundsson M, El-kwae EA, Kabuka MR. Edge detection in medical images using a genetic algorithm. IEEE Trans Med Imaging 1998;17:469–474.
26. Canny JF. A computational approach to edge detection. IEEE Trans Pattern Anal Mach Intell 1986;8: 679–698.
27. Russ JC. Image processing handbook, 2nd ed. CRC Press; 1995. p 225–262.
28. Parker JR. Algorithm for image processing and computer vision. John Wiley; 1997. p 1–66.
29. Rekeczky C, Schultz A, Szatmari I, Roska T, Chua LO. Image segmentation and edge detection via constrained diffusion and adaptive morphology: A CNN approach to bubble/debris image enhancement. Proc Int Symp Nonlinear Theory & Applications, p 209–212, Hawaii, 1997.
30. Aizenberg IN, Aizenberg NN, Vandewalle J. Precise edge detection: Representation via Boolean functions, implementations on the CNN. Proc IEEE Int Workshop Cellular N. N. and Their Applications, p 301–306, London, 1998.
31. Rekeczky C, Roska T, Ushida A. CNN-based difference-controlled adaptive nonlinear image filters. Int J Circuit Theory Appl 1998;26:375–423.
32. Abrantes AJ, Marques JS. Unified approach to Snakes, elastic nets and Kohonen maps. Proc IEEE ICASSP, p 3427–3430, 1995.
33. Nagai H, Miyanaga Y, Tochinai K. An edge detection by using self-organization. Proc IEEE ICASSP, p 2749–2752, 1998.
34. Guan L, Perry SW, Romagnoli R, Wong H, Kong H. Neural vision system and applications in image processing and analysis. Proc IEEE ICASSP, p 1245–1248, 1998.
35. Toivanen PJ, Ansamaki J, Leppajarvi S, Parkkinen JPS. Edge detection of multispectral images using the 1-D self organizing map. Proc Int Conf Artificial Neural Networks, p 737–742, Skovde, Sweden, 1998.
36. Bhuiyan MS, Sato M, Fujimoto H, Iwata A. Edge detection by neural network with line process. Proc Int Joint Conf Neural Networks, p 1223–1226, 1993.
37. Bhuiyan MS, Sato M, Fujimoto H, Iwata A. An improved neural network based edge detection method. Proc Int Conf Neural Inf Process Seoul 1994;1:620–625.
38. Iwata H, Agui T, Nagahashi H. Boundary detection of color images using neural networks. Proc IEEE ICNN, p 1426–1429, 1995.
39. Muneyasu M, Hotta K, Hinamoto T. Image restoration by Hopfield networks considering the line process. Proc IEEE ICNN, p 1703–1706, 1995.
40. Ohashi G, Oya A, Natori M, Nakajima M. Edge extraction method using neural network for three dimensional display of ultrasonic echo image. Trans IEICE 1993;J76-D-II:368–373.
41. Coppini G, Poli R, Valli G. Recovery of the 3-D shape of the left ventricle from echocardiographic images. IEEE Trans Med Imaging 1995;14:301–317.
42. Ueda K, Yamada M, Horiba I, Ikeya K, Suzuki K. A direct estimation method of occupancy rate in parking lot using analogue output neural network model. Trans Inf Process Soc 1995;36:627–635.
43. Rumelhart DE, Hinton GE, Williams RJ. Learning internal representations by error propagation. In Parallel distributed processing, Vol 1. MIT Press; 1986. p 318–362.
44. Suzuki K, Horiba I, Ikeya K, Nanki M. Artifact reduction method in cardiac DSA. 1992 Tokai Joint Meeting, p 351.
45. Otsu N. A threshold selection method from gray-level histograms. IEEE Trans Syst Man Cybern 1979;9: 62–66.
46. Oppenheim AV, Schafer RW. Digital signal processing. Prentice–Hall; 1975.
47. Duda RO, Hart PE. Pattern classification and scene analysis. Wiley; 1971. p 267–272.
48. Suzuki K, Horiba I, Ikeya K, Nanki M. Recognition of coronary artery stenosis using neural network on DSA system. Trans IEICE 1994;J77-D-II:1910–1916.
49. Trobaugh GB, Hallstrom AP, Kennedy JW. Reproducibility of ventricular function measurements by contrast angiography. Catheterization and Cardiovascular Diagnosis 1984;10:561–572.
50. Suzuki K, Horiba I, Sugie N. Designing the optimal structure of a neural filter. In Niranjan M, et al (editors). Neural networks for signal processing VIII. IEEE; 1998. p 323–332.
51. Suzuki K, Horiba I, Sugie N. A method for determining reduced structure of a neural filter. Trans Inf Process Soc 1999;40:4226–4238.
52. Funahashi K. On the approximate realization of continuous mappings by neural networks. Neural Networks 1989;2:183–192.

53. Barron AR. Universal approximation bounds for superpositions of a sigmoidal function. IEEE Trans Inf Theory 1993;39:930–945.
54. Mori S, Sakakura T. Fundamentals of image recognition [II]. Part IV. Edge detection. Ohm Press; 1990. p 97–184.
55. Marr D, Hildreth E. Theory of edge detection. Proc R Soc London 1980;207:187–217.
56. Hueckel MH. An operator which locates edges in digitized pictures. J ACM 1971;18:113–125.
57. Suzuki K, Horiba I, Sugie N. Efficient approximation of a neural filter for quantum noise removal in X-ray images. In Hu Y-H, et al (editors). Neural networks for signal processing IX. IEEE; 1999. p 370–379.
58. Suzuki K, Horiba I, Sugie N. An analysis of the neural filter trained to improve quality of images with quantum noise and realization of approximate filter. Trans Inf Process Soc 2000;41:711–721.
59. Rigaud M, Hardy A, Castadot M, Rocha P, Dubourg O, Delorme G, Bardet J, Bourdarias JP. Variability and reproducibility of quantitative left ventricular angiography. Catheterization and Cardiovascular Diagnosis 1989;16:8–15.
60. Okabe T, Uritani T (editors). Iyo Gazo Kogaku (Medical image engineering). Ishiyaku Shuppan; 1997. p 148–149.
61. Loertscher R, Burkart F, Schmitt HE, Emmenegger H. Reproducibility of left ventricular volume determinations with use of a semi-automated system. Cardiovascular and Interventional Radiology 1984;7:53–58.
62. Kass M, Witkin A, Terzopoulos D. Snakes: Active contour models. Int J Computer Vision 1988;1:321–331.

AUTHORS (from left to right)

Kenji Suzuki (member) received his B.S. and M.S. degrees, both with honors, in electrical and electronic engineering from Meijo University in 1991 and 1993, and Ph.D. degree in information engineering from Nagoya University in 2001. From 1993 to 1997, he was with the Research and Development Center at Hitachi Medical Corporation as a researcher. He was engaged in research and development of intelligent medical imaging systems, including a digital subtraction angiography system and a digital radiography system. In 1997, he joined Aichi Prefectural University, and assisted in founding the Faculty of Information Science and Technology. From 1998 to 2002, he was with that Faculty as a research associate. From 2001 to 2002, he was with the Kurt Rossmann Laboratories for Radiologic Image Research, Department of Radiology, Division of Biological Sciences, University of Chicago, as a visiting research associate. Since 2002, he has been a research associate at the Laboratories. His research interest includes medical image processing and recognition, and neural networks. He is a member of IEEE, Information Processing Society, IEE Japan, Japanese Neural Network Society, and Japanese Circulation Society.

Isao Horiba (member) received his B.S. and Ph.D. degrees in electrical engineering from Nagoya University in 1974 and 1985. From 1974 to 1987, he was a senior researcher with the Research and Development Center at Hitachi Medical Corporation. He was engaged in development of computed topography systems, and in research and development of many kinds of medical imaging systems, including magnetic resonance imaging systems, digital subtraction angiography systems, and digital radiography systems. In 1987, he joined the Faculty of Science and Technology at Meijo University as an assistant professor, and later became an associate professor. He was appointed a professor on the Faculty of Information Science and Technology at Aichi Prefectural University in 1998, and has been a professor in the Graduate School of Information Science and Technology since 2002.

AUTHORS (continued) (from left to right)

Noboru Sugie (fellow) received his B.S. degree in electrical engineering from Nagoya University in 1957, and Ph.D. degree in engineering from the University of Tokyo in 1970. From 1957 to 1979, he was with the Government Electrotechnical Laboratory. During the period from 1962 to 1964, he was on leave at the Department of Electrical Engineering, McGill University, Montreal, Canada, as an NRC postdoctoral fellow. He was the director of the sections of both bionics and human vision at the Government Electrotechnical Laboratory, from 1970 to 1977 and from 1977 to 1978, respectively. From 1979 to 1994, he was a professor in the Department of Information Engineering and the Graduate School of Engineering at Nagoya University. From 1990 to 1994, he was also the director of the Nagoya University Computation Center. He is now a professor emeritus of Nagoya University. From 1994 to 2000, he was a professor in the Department of Electrical and Electronic Engineering and the Graduate School of Science and Technology at Meijo University. Since 2000, he has been the founding chairman of the Department of Information Sciences and Technology.

Michio Nanki received his M.D. degree from Nagoya University in 1976. From 1976 to 1979, he was with Shizuoka Saiseikai Hospital. From 1979 to 1982, he was with the cardiovascular division of the Third Department of Internal Medicine at Nagoya University. From 1982 to 1984, he was with the cardiovascular division at the National Cardiovascular Center. He was a Vice Director from 1985 to 1996, and a Chief Director from 1996 to 2000 of the cardiovascular division at Chubu Rosai Hospital. Since 2000, he has been a Vice President of Chubu Rosai Hospital.